Photodynamics and Surface Characterization of TiO_2 and Fe_2O_3 Photocatalysts Immobilized on Modified Polyethylene Films

M. R. Dhananjeyan,[†] E. Mielczarski,[⊥] K. R. Thampi,[†] Ph. Buffat,[‡] M. Bensimon,[§] A. Kulik,[∥] J. Mielczarski,[⊥] and J. Kiwi*,[†]

Department of Chemistry, Laboratory of Photonics and Interfaces, Institute of Electron Microscopy, Department of Civil Engineering, and Department of Physics, Institute of Atomic Engineering, Swiss Federal Institute of Technology, CH-1015 Lausanne, Switzerland, and Laboratory LEM/UMR 7569, CNRS INPL-ENSG, BP40, 54501 Vandoeuvre les Nancy Cedex, France

Received: April 10, 2001; In Final Form: August 16, 2001

Polyethylene block-copolymer films containing negative anhydride groups were used to immobilize TiO_2, Fe_2O_3, and Fe^{3+} photocatalysts. The kinetics of the mineralization of azo-dye Orange II and chlorophenols on copolymer−TiO_2, copolymer−Fe_2O_3, and copolymer−Fe^{3+} have been tested under optimized experimental conditions. In the case of copolymer−TiO_2, the degradation kinetics for the model organic compounds were about the same as those observed with TiO_2 suspensions containing about a 27 times higher amount of TiO_2 per unit volume. The surface of the derivatized copolymer semiconductor catalysts was studied by infrared attenuated total reflection spectroscopy. The spectroscopic data provided evidence for a TiO_2 interaction with the negatively charged conjugated carboxylic groups of the copolymer, leading to an asymmetric-stretching band of $-COO-Ti^{4+}$ at the position expected for metal carboxylates. In the case of Fe_2O_3 and Fe^{3+}, the asymmetric-stretching carboxylate bands are ascribed to the carboxylate bands of $-COO-Fe_2O_3$ and $-COOO-Fe^{3+}$. Evidence is presented by X-ray photoelectron spectroscopy for the existence of two oxidation states of Ti and Fe after the photocatalytic degradation of Orange II. This observation is consistent with light-induced interfacial charge transfer (redox processes) taking place at the metal−oxide copolymer surface. The nature of the latter processes is presented in detail during this study.

Introduction

During the past decade, heterogeneous photocatalysis has been increasingly used in the preparation of fine chemicals and in water and air purification. More than 1360 references have appeared during the last 10 years in internationally reviewed journals where TiO_2[1−10] and Fe_2O_3[11] are used as photocatalysts. However, two major obstacles hinder the TiO_2 photocatalytic performance of these semiconductors in suspension: (a) the separation of the semiconductor catalyst after the treatment and (b) the low quantum efficiency of these processes. This study addresses the first issue, namely, the anchoring of TiO_2, Fe_2O_3, and Fe^{3+} on copolymers to avoid the costly separation of the suspensions after treatment. Supported titania-coated glass has been reported during the past decade and led to catalyst dissolution[12,13] during the degradation of pollutants. More recently, Nafion−Fe catalytic membranes have been shown to be effective as photocatalysts and resistant to the attack of OH radicals with adequate kinetics and stability during long-term operation.[14] However, Nafion is too expensive to be used as a catalyst support in large-scale applications. The present study presents a new copolymer[15,16] with TiO_2 or Fe_2O_3 immobilized on its surface that is able to (a) withstand reactive radical attack during light irradiation in an oxidative media, (b) maintain adequate long-term catalytic stability, and (c) preclude semiconductor leaching during the degradation process. Derivatized polyethylene has been selected because polyethylene is the most inert polymer material from DuPont after Teflon.

The catalytic performance and characterization of these new materials will be explored during the degradation of a model azo-dye (Orange II) and some common chlorocarbons. Nonbiodegradable azo-dye Orange II is widely used in the textile industry. It is resistant to bacterial treatment; therefore, biological degradation cannot be employed to abate this compound.[3] The TiO_2-mediated degradation of Orange II[4] and other azo-dyes, such as Rose Bengal[5] and Eosin,[6] is a field of active research.

The removal of chlorophenols on TiO_2 semiconductor suspensions under light irradiation has been widely reported during the past decade[1,2,7−9] because they are EPA priority pollutants. The degradation of 2,4-dichlorophenol (2,4-DCP) mediated by TiO_2 suspensions under light has been recently reported.[10,11] Because of the long time needed for biological degradation, 2,4-DCP goes unabated through biological treatment stations and gives rise to a serious environmental problem.

During this study, the catalyst performance will be shown to depend on the suitable combination of (a) the type of the semiconductor applied on the copolymer surface, (b) the oxidant leading to the most effective separation, and (c) the radiation frequency and intensity of the lamp source. Both O_2 and H_2O_2 have been used as oxidants for the reactions. In the case of copolymer−Fe_2O_3, H_2O_2 is the only effective oxidant, whereas in the case of copolymer−TiO_2, O_2 was able to carry out the oxidation reaction.

[†] Department of Chemistry, Laboratory of Photonics and Interfaces, Swiss Federal Institute of Technology.
[⊥] Laboratory LEM/UMR 7569, CNRS INPL-ENSG.
[‡] Institute of Electron Microscopy, Swiss Federal Institute of Technology.
[§] Department of Civil Engineering, Swiss Federal Institute of Technology.
[∥] Department of Physics, Institute of Atomic Engineering, Swiss Federal Institute of Technology.

10.1021/jp011339q CCC: $20.00
Published on Web 11/08/2001

Experimental Section

Chemicals. Orange II, 2-chlorophenol, 4-chlorophenol, 2,4-DCP, and H_2O_2 were Fluka p.a. and used as received. Triple-distilled water was used in all of the experiments. Titania TiO_2 P-25 Degussa (50 m^2/g) was deposited on polyethylene−maleic anhydride block-copolymer films (DuPont Co.; 30 μm thick) by the procedure outlined as follows.[15,16]

Preparation of the Semiconductor-Loaded Copolymer. The immobilized anhydride-derivatized polyethylene−TiO_2 was prepared in the following way. First, the polyethylene film was thoroughly washed with water. Then, the membrane was dipped in a TiO_2 P-25 suspension (5 g/L) for several hours. This titania suspension was heated for 1 h at 75 °C in the presence of the polyethylene copolymer, and subsequently, the copolymer−TiO_2 film was taken out and dried at 100 °C for 1 h. The copolymer film was then washed to eliminate the loosely bound TiO_2 particles. The final copolymer film had a titania loading of 1.5 mg spread on a 48 cm^2 area of the copolymer (100 mg). The titania deposition could be reproduced on the copolymer film within ±15% accuracy by weight of the deposited TiO_2. The hematite−copolymer samples were prepared similarly using hematite instead of TiO_2. For the anchoring of Fe^{3+}, $FeCl_3$ (Fluka) was used as the starting material.

Photoreactor and Irradiation Procedures. The irradiation vessels were 60 mL cylindrical Pyrex flasks (cutoff 290 nm) each containing 40 mL of a reagent solution. Copolymer strips of 48 cm^2 were placed immediately behind the wall of the reaction vessel. The titania suspensions as well as the copolymer−TiO_2 strips were irradiated in the UV region using a medium-pressure 125 W mercury lamp (360° radiation field at $\sim 2.5 \times 10^{15}$ photons/s) from Photochemical Reactors Limited, Berkshire, U.K. The main irradiation wavelength of the mercury lamp was 366 nm, and the light of <290 nm was cut by the batch reactor Pyrex wall.

The irradiation of polymer−Fe_2O_3 was carried out in the visible region in the cavity of a Hanau Suntest solar simulator air-cooled at 46 °C. The Suntest lamp had a wavelength distribution with about 7% of the photons between 290 and 400 nm. The profile of the photons emitted between $\lambda = 400-800$ nm followed the solar spectrum. The Suntest solar simulator had an intensity of 80 mW/cm^2 within the wavelength range of 290 and 800 nm. The radiant flux in mW/cm^2 was measured with a power meter from LSI Corp., Yellow Springs, CO.

Photolysis of Solutions. The detection of Fe^{3+} in solution was carried out by complexing the Fe^{3+} ion in solution with thiocyanate and the Fe^{2+} ions with phenanthroline. Spectrophotometric analyses of the solutions were carried out with a Hewlett-Packard 8452 diode array spectrophotometer. The total organic carbon (TOC) was monitored via a Shimadzu 500 instrument equipped with an automatic sample injector. Dye degradation was followed by a Varian HPLC provided with a 9065 diode. A Phenomenex C-18 inverse-phase column was used, and the dye signals were detected at 229 and 254 nm. The gradient solution was regulated with a buffer consisting of ammonium acetate and methanol. The peroxide concentration in the solution was followed by Merkoquant paper at levels between 0.5 and 25 mg/L of H_2O_2 in the aqueous solution.

X-ray Photoelectron Spectroscopy (XPS). The XPS spectra were obtained with a multidetection electron-energy analyzer (VSW FAT mode CL 150). The monochromatic magnesium radiation source (1253.6 eV) was operated at 15 kV and 10 mA. The XPS resolution between 0.9 and 1.0 eV was determined by the use of a gold standard. The operating pressure of the spectrometer analyzer chamber was close to 10^{-8} mbar. The measurement was performed with a takeoff angle close to 90°. High charging effects on the samples were observed at 2 and 4 eV. The carbon 1s line (284.6 eV) was used as a reference to correct the charging effects. The characteristic peaks of Ti 2p, Fe 2p, O 1s, and C 1s, were recorded in the appropriate range of the binding energies in order to obtain a good signal-to-noise ratio for the best resolution of the recorded spectra. The recorded lines were smoothed by a polynomial fit and background subtraction according to Shirley[17] and then fitted using a curve-fitting program provided with a Gaussian and Lorentzian curve generator.

Infrared Attenuated Total Reflection (IRATR) Fourier Transform Spectroscopy. This technique was applied to study the surfaces of the unloaded and loaded copolymer−TiO_2, copolymer−Fe_2O_3, and copolymer−Fe^{3+}. The reflection spectra were recorded on a Bruker IFS 55 FTIR spectrophotometer equipped with a mercury cadmium telluride detector and an internal reflection attachment from Harrick Co. The detailed description of the applied ATR technique can be found in ref 18. The polyethylene samples were contacted with a ZnSe reflection element with dimensions of 50 × 20 × 3 mm and an incident angle (Θ) of 45°. The depth of penetration (d_p) of incident radiation, defined as the distance required for the electric-field amplitude to fall to e^{-1}, is calculated from

$$d_p = \lambda_1/2\prod(\sin^2\Theta - n_{21}{}^2)^{1/2} \qquad (1)$$

The refraction index used was $n_2 = 1.4$ for polyethylene and $n_1 = 2.4$ for the reflection of the elements. This allowed for an estimation of 2.3 μm for the penetration depth at a wavenumber of 1700 cm^{-1}. The reflection spectra were recorded for both sides of each copolymer sample, showing no differences.

High-Resolution Inductively Coupled Plasma Spectrometry (ICPS). The samples were acidified with nitric acid and diluted in ultrapure water. The experiments were directed toward the determination of the Ti^{4+} ion in the irradiated solutions. The ion beam in the plasma of the instrument (Micromass, U.K.) was directed through the sampling interface and then accelerated into the mass analyzer. The collector assembly is a dual-detector system provided with a Faraday cup for the high-beam current coupled with an electron-multiplier amplifier for the low-intensity signals. To overcome the overlap interference problems, measurements were referenced to a mass resolution of 3500.

Transmission Electron Microscopy (TEM) and Diffraction Measurements. A Philips EM 430 Twin (300 kV and 2.3 Å point resolution) instrument was used for TEM and diffraction measurements. The samples were prepared by ultramicrotomy using a diamond knife (45° edge) to cut them into thin slices, and then the samples were subsequently embedded in an Embed 812 epoxy resin. Different cutting geometries were tried for the softer polymer oxide loaded samples.

Gas Adsorption Studies. Gas physisorption was carried out using a Sorptomatic 1990 Micropore unit. The adsorption isotherms were reproducible to 2%. The experiments were performed at the liquid-nitrogen boiling temperature (77 K). The surface area of the samples was evaluated with the help of a 19190 Micropore computer system.

Results and Discussion

Decoloration and Degradation of Orange II on Copolymer−TiO_2 Membranes. Figure 1 presents the UV−vis spectra of the copolymer alone and copolymer−TiO_2. The increase in the absorbance on the copolymer is due to the deposited TiO_2.

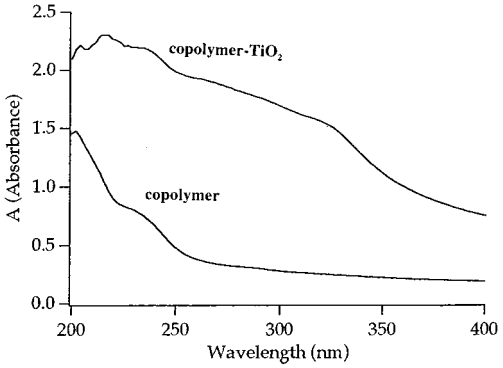

Figure 1. Absorption spectra of the copolymer and of the TiO_2-coated copolymer.

Without the presence of copolymer−TiO_2, the decoloration of Orange II (0.1 mM) by H_2O_2 (10 mM) under mercury-lamp irradiation did not proceed. The results indicate that catalytic sites at the surface of titania, whether in a suspended or an immobilized form, are responsible for the abatement of Orange II. In the dark, no decrease in the Orange II absorbance was observed.

Figure 2a shows the result of the decoloration of Orange II using titania suspensions and that of copolymer−TiO_2 in the presence of H_2O_2 under medium-pressure mercury light (400 W) and in the dark. The peroxide in the solution decreased from initially 340−25 mg/L after 6 h.

Figure 2b shows that the decrease in TOC under the irradiation of Orange II on copolymer−TiO_2 proceeds to a level of 8 mg of C/L. The shoulder that sets in after 4 h of degradation in Figure 2b does not correspond to copolymer decomposition under light irradiation resulting from the H_2O_2 present, as indicated by control experiments. The shoulder is due to the nondegradable intermediates generated during the degradation of Orange II under light. The upper trace in Figure 2b shows the formation of nondegradable intermediates in the dark, precluding further decomposition of Orange II. This is in agreement with previous work with TiO_2 suspensions.[4,14,16,18−20] The reduction in TOC is seen to be slower than the Orange decoloration shown in Figure 2a. Figure 2b shows that the decrease in TOC of Orange II under light irradiation is higher when TiO_2 suspensions are used. It should be noted that the concentration of titania is about 27 times higher in the suspension when compared to the amount anchored on the polymer.

Orange II has been reported to act as the photosensitizer of the surface bound TiO_2. The low-energy edge of Orange II has been reported to be 565 nm or 2.3 eV.[19] The photosensitization of Orange II on copolymer−TiO_2 leads to a charge transfer with the concomitant quenching of Orange II* and the formation of Orange $II^{\bullet+}$ (eq 2). The latter species is documented in the literature.[19,20] On thermodynamic grounds, charge transfer from

$$\text{Orange II} + \text{copolymer}-TiO_2 + h\nu \rightarrow [\text{Orange II}^*...TiO_2]\text{copolymer} \rightarrow \text{Orange II}^{\bullet+} + \text{copolymer}-TiO_2 + e^-_{cb} \quad (2)$$

Orange II in the excited state to TiO_2 is possible. On the basis of cyclic voltammetry, an oxidation potential of 0.76 V (NHE) was reported for Orange II.[20] Because the low-energy absorption edge of Orange II is 2.3 eV, the excited-state standard potential of Orange II can be estimated [from the energy gap between the ground sate and the excited state ($\Delta G°$)] of Orange II to be −1.54 eV.[21] Therefore, the electron transfer from the excited state of the dye to the conduction band of TiO_2 at −0.1 eV is thermodynamically possible. This is shown in Scheme 1.

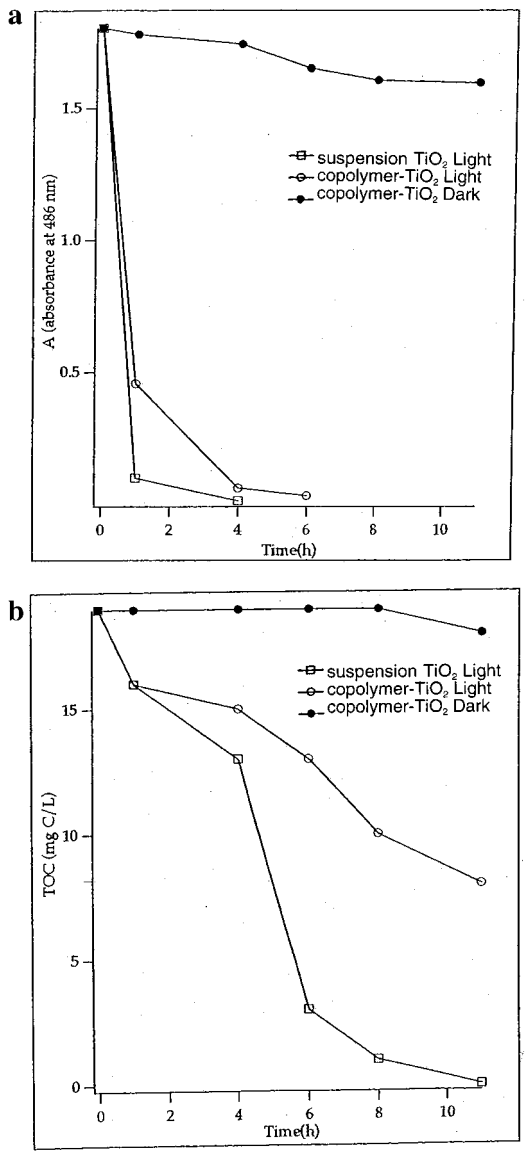

Figure 2. (a) Absorbance of Orange II (0.1 mM) during the decoloration at a pH of 6 in the presence of H_2O_2 (10 mM) under medium-pressure mercury-lamp irradiation. The supported catalyst was copolymer−TiO_2, and the suspensions of the TiO_2 catalyst were 1 g/L. (b) TOC decrease of Orange II solutions up to 10 h irradiation time with the same copolymer and experimental conditions as those used in part a.

IR and XPS Characterization of Copolymer and Copolymer−TiO_2 before and after Photodegradation of Orange II. IR spectra of the copolymer and the loaded copolymer−TiO_2 polymer before and after the photodegradation of Orange II are presented in Figure 3. The band assignments are listed in Table 1 and indicate that the TiO_2 is immobilized on the copolymer through carboxyl groups. The reflection spectrum of copolymer−TiO_2 shows the growth of bands at 1541 and 1415 cm^{-1} (Figure 3b). These bands correspond to the asymmetric- and symmetric-stretching vibrations of the carboxylate groups. The position of the bands characteristic for metal carboxylates reported in Figure 3 have been well documented in the literature.[22−26] Concomitantly, the band at 1793 cm^{-1} due to the anhydride carboxylic groups disappears (Figure 3a). The frequency difference ($\Delta\nu$) between the asymmetric- and symmetric-stretching vibrations of the carboxylate group can be correlated with the

SCHEME 1

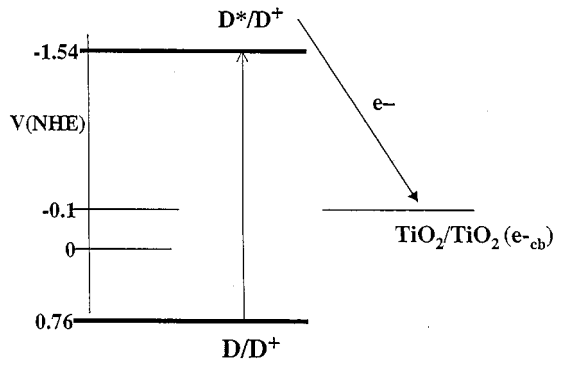

coordination mode of the carboxylate ligand.[24,25] The calculated $\Delta\nu$ parameter is 126 cm^{-1} and indicates the formation of a bidentate ligand between polymer carboxyl groups and the surface titanium atoms, according to the literature.[25,26] The distinction between chelation or bridging surface complex formation is difficult in this case without other supporting information.

Other observed differences in spectra a−c in Figure 3 consist of the shift from 1300 to 1280 cm^{-1} of the broad band resulting from the coupled vibration of C−O and OH groups. Further, a lower intensity for the OH deformation band was observed at 909 cm^{-1}. These observations support the conclusion that a carboxyl−titanium complex is formed when TiO_2 particles are loaded on the copolymer. It should also be noted that there are still a significant number of carboxylic groups left on the copolymer, as shown by the band at 1714 cm^{-1}, that are not involved in binding with the titanium atoms from the loaded particles. A new band was also observed at 1640 cm^{-1}, indicating water adsorption on the loaded TiO_2 particles. This suggests that water adsorbs on TiO_2 though they also strongly interact (chemisorb) with the copolymer surface. The strong increase in absorption below 850 cm^{-1} (Figure 3b) is characteristic of the vibrations of TiO_2. The higher frequency vibration is due to the displacement of Ti^{4+} relative to the O^{2-} ions along the *c* axis[24] immobilized on the copolymer surface.

The reflection spectrum of copolymer−TiO_2 after Orange II degradation (Figure 3c) shows features almost identical to those found for copolymer−TiO_2 before use (Figure 3b). The more intensive bands at 1017 and 1046 cm^{-1} are assigned to the C−O stretching vibration of the intermediates produced during photocatalytic degradation. The amount of the adsorbed intermediates on copolymer−TiO_2 is very low, suggesting that a decrease in catalyst efficiency with time will also be very low or will not take place at all. Another assignment of the two low-intensity bands is related to the stretching vibration of the C−O groups of the surface carboxylate groups. With the latter assignment, any significant adsorption of the intermediates during a catalytic reaction is excluded, suggesting a good catalytic efficiency of the copolymer−TiO_2 catalyst.

The samples investigated by IR were also characterized by XPS, taking the TiO_2 P-25 Degussa powder as reference sample. The results obtained are presented in parts a and b of Table 2. Analysis of the results led to a few interesting observations. The most interesting are probably the presence of two oxidation states (Figure 4) of surface titanium species, two doublets of Ti 2p with an intensity ratio of 1:2, and a splitting of about 5.7 eV[27] in samples after the photodegradation of Orange II. The major component is Ti^{4+}, typical of TiO_2 powder, but also ~35% of the total titanium surface atoms are in the Ti^{3+} state (see Figure 4 and Table 2b). This observation supports the

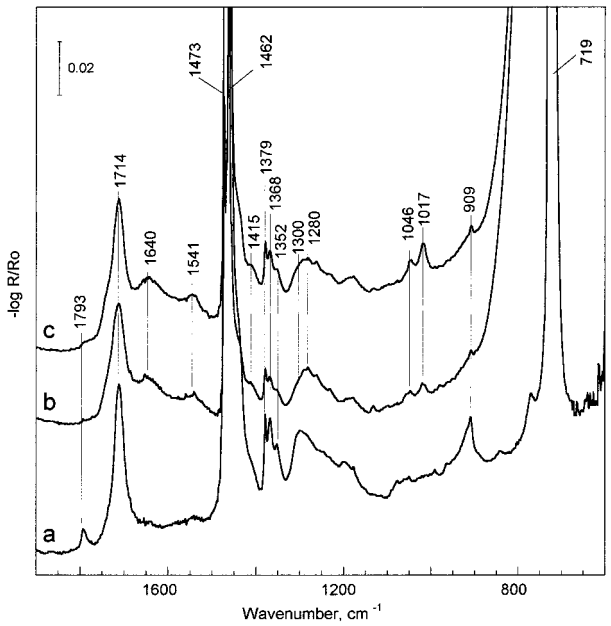

Figure 3. Attenuated total reflection infrared spectra of (a) copolymer alone, (b) copolymer−TiO_2 before use, and (c) copolymer−TiO_2 after Orange II degradation at a pH of 6 with visible-light irradiation.

conclusion that, during photodegradation, titanium changes its oxidation state. Another finding (Table 2) is that the surface of the TiO_2 particle on the copolymer is more strongly hydroxylated, as reflected in the OH-surface component observed at 531.6 eV compared to the initial P-25 Degussa sample. The intensity of the surface hydroxyl groups is very high compared with that of the oxygen signal in TiO_2 at 529.5 eV. Through these surface hydroxyl groups, Orange II interacts with TiO_2 and undergoes photocatalytic decomposition.

IR and XPS Characterization of Copolymer−Fe_2O_3 before and after Degradation of Orange II. IRATR spectra of the loaded Fe_2O_3 polymer before and after the photodegradation of Orange II and the band assignments are reported in Table 1. Fe_2O_3 is immobilized on the copolymer through carboxyl groups. The corresponding band at 1520 cm^{-1} is very weak in the spectrum of the nonloaded copolymer. The reflection spectra of polymer−Fe_2O_3 samples show new bands at 1567 cm^{-1} and a stronger band at 1520 cm^{-1}, and the latter two bands are assigned to the asymmetric-stretching vibrations of the carboxylate groups. Close to the strong $-CH_2$ deformation band at 1462 cm^{-1}, a weak shoulder at about 1415 cm^{-1} is also observed. This shoulder is due to the symmetric-stretching vibrations of the carboxylate groups. At the same time, the band at 1793 cm^{-1} assigned to carboxyl anhydride almost disappears. These observations indicate that an iron−carboxylate surface complex is bonding the Fe_2O_3 particles to the copolymer surface.

Two bands at 1567 and 1520 cm^{-1} are observed and assigned to the asymmetric-stretching vibrations of the carboxylate groups, suggesting two conformations of carboxylate groups as reported for the calcium−oleate surface complex.[28] The formation of mixed valance $Fe^{2+}-Fe^{3+}$ complexes should also be considered during carboxylate surface complex formation. The calculated $\Delta\nu$ parameters for the observed asymmetric- and symmetric-carboxylate vibrations are 152 and 105 cm^{-1}, respectively. According to the literature,[24,25] values of $\Delta\nu$ lower than 200 cm^{-1} are indicative of chelation or bridging formation. Both of them could be suggested as responsible for the strong attachment of the Fe_2O_3 particles to copolymer surfaces.

Similarly, as for the copolymer−TiO_2 sample, a new band at 1640 cm^{-1} is observed, indicating a significant water

TABLE 1: Assignment of Absorbance Bands on the Copolymer, Copolymer−TiO_2, Copolymer−Fe_2O_3, and Copolymer−Fe^{3+} before and after Degradation of Orange II[a]

virgin polymer	polymer with TiO_2	polymer with TiO_2 after Orange II decomposition	polymer with Fe_2O_3	polymer with Fe_2O_3 after Orange II decomposition	polymer with Fe^{3+}	polymer with Fe^{3+} after Orange II decomposition	assignment
−	∼3340 w broad	∼3340 w broad	3386	3386	3473 vs, 3363 vs	3473 vs, 3363 vs	OH stretching
2915 vs	i	i	i	i	i	i	CH_2 asymmetric stretching
2847 vs	i	i	i	i	i	i	CH_2 asymmetric stretching
1793 w	−	−	−	−	−	−	carboxyl (anhydrite)
1714 s	i	i	i	i	i	i	carboxyl group
−	1640	i	i	i	i	i	adsorbed water
	1541	1541	1567, 1520	1567, 1520	1594, 1560, 1523	1594, 1560, 1523	carboxylate asymmetric stretching metal complex
1473 vs	i	i	i	i	i	i	CH_2 deformation
1462 vs	i	i	i	i	i	i	CH_2 deformation
−	1415	i	i	i	i	i	carboxylate symmetric stretching
1379 w	−	−	−	−	−	−	CH_3 deformation
1368 w	i	i	i	i	i	i	CH_3 deformation
1352 w	i	i	i	i	i	i	CH deformation
∼1300 w broad	1280	1280	1285	1285	1300, 1250	1300, 1250	coupled CO stretching and OH in-plane deformation
−	1046, 1017	1046, 1017	1048, 1016	1016	1047, 1018	1047, 1018	CO stretching of carboxylate group
909	i	i	i	i	i	i	OH out-of-plane deformation
below 850 vs	below 850 vs	below 850 vs	below 780 vs	below 780 vs	829 broad	829 broad	absorbance due to Me−O stretching of loaded catalysts
719 vs	i	i	i	i	i	i	C−C skeletal vibration

[a] According to refs 22−26. Key to abbreviations: (−) band not observed, (i) same position as in previous column, (vs) very strong, (s) strong, (w) weak.

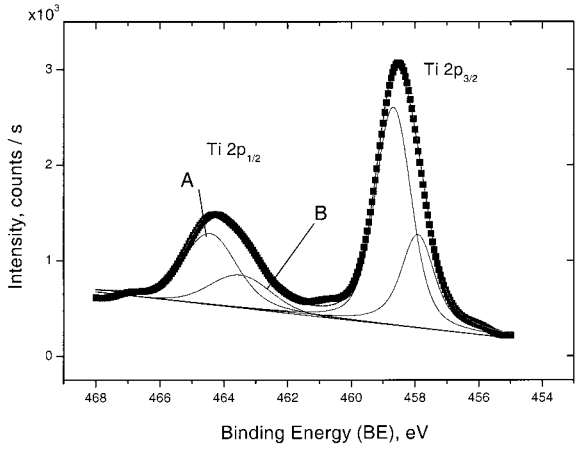

Figure 4. XPS spectrum of copolymer−TiO_2 after degradation of Orange II (Ti 2p line). Component A is characteristic for TiO_2, whereas component B is due to Ti^{3+} surface species.

adsorption on the loaded Fe_2O_3 particles. The strong increase in absorption below 780 cm^{-1} is characteristic for the vibrations of Fe_2O_3 immobilized on the copolymer surface.[24]

The reflection spectrum of copolymer−Fe_2O_3 after Orange II degradation shows spectral features similar to those of the copolymer−Fe_2O_3 before use. There is a difference in the spectral region at about 1000 cm^{-1} in which the band assignment is somewhat difficult. Assuming that the low-intensity bands at 1016 and 1045 cm^{-1} are due to the C−O stretching vibration of an iron−carboxylate surface complex, the observation of a new band at 985 cm^{-1} and the disappearance of the band at 1048 cm^{-1} suggest the adsorption of intermediates produced during the photocatalytic degradation of Orange II. The amount of the adsorbed intermediates on the copolymer−Fe_2O_3 catalyst is very low; therefore, it is expected that the decrease of the catalytic efficiency with time will also be very low.

TABLE 2: Binding Energy of Ti 2p, O 1s, and C 1s Elements and Atomic Surface Concentration of Detected Elements for TiO_2 Catalysts

(a) Binding Energy (eV)

sample	Ti $2p_{1/2}$		Ti $2p_{3/2}$		O 1s			C 1s
TiO_2 powder	458.3		464.0		533.1	531.6	529.5	284.6
polymer−TiO_2 before use	458.5		464.2		533.4	531.9	529.7	284.6
polymer−TiO_2 after use in degradation of Orange II	458.5	458.0	464.2	463.6	533.4	531.9	529.8	284.6

(b) Atomic Surface Concentration (%)

sample	Ti		O			C
	Ti^{4+}	Ti^{3+}	H_2O_{ads}	OH_{surf}	O_{oxides}	
TiO_2 powder	10.1		3.3	7.0	21.6	57.8
polymer−TiO_2 before use	4.7		1.7	9.7	12.7	71.1
polymer−TiO_2 after use in degradation of Orange II	2.25	1.25	1.4	10.7	9.6	74.5

The XPS results of the copolymer−Fe_2O_3 samples before and after use in the Orange II photodegradation and also of the Fe_2O_3

TABLE 3. Binding Energy of Ti 2p, O 1s, and C 1s Elements and Atomic Surface Concentration of Detected Elements for Fe_2O_3 Catalysts

(a) Binding Energy (eV)

sample	Fe $2p_{1/2}$	Fe $2p_{3/2}$	O 1s			C 1s
Fe_2O_3 powder	710.9	724.6	532.8	531.3	529.6	284.6
polymer−Fe_2O_3 before use	711.3	725.0	532.6	531.1	529.4	284.6
polymer−Fe_2O_3 after use in degradation of Orange II	711.1	724.8	531.1	531.6	529.8	284.6

(b) Atomic Surface Concentration (%)

	Fe 2p		O			
sample	Fe^{2+}	Fe^{3+}	H_2O_{ads}	OH_{surf}	O_{oxides}	C
Fe_2O_3 powder	10.7					
	56%	44%	4.4	7.9	17.5	59.8
polymer−Fe_2O_3	1.4					
before use	58%	42%	11.6	9.6	0.9	76.5
polymer−Fe_2O_3	7.8					
after use in degredation of Orange II	46%	54%	0	6.8	14.8	70.7

reference powder are shown in parts a and b of Table 3. The most striking difference is the nearly 5 times higher intensity of the Fe 2p line for the copolymer−Fe_2O_3 sample after Orange II degradation compared to the unused copolymer−Fe_2O_3. This is seen in Table 3b, where 10.7, 1.4, and 7.8 represent the total concentration of Fe on the surface for the Fe_2O_3 powder and copolymer−Fe_2O_3 before and after use, respectively. Concomitantly, the O 1s line undergoes very strong variations. The unused copolymer−Fe_2O_3 shows very strong oxygen components at 532.6 and 531.1 eV, characteristic for the adsorbed water and the surface OH groups, while the oxygen component at 529.4 eV due to Fe_2O_3 is seen to be almost negligible. This indicates that the Fe_2O_3 surface is strongly hydrated after loading the iron oxide on the copolymer. After the copolymer−Fe_2O_3 mediates Orange II photodegradation, the opposite is observed. The O 1s oxide component at 529.8 eV is the dominating one, whereas the OH component is much lower with no presence of adsorbed water (component at ∼533 eV). The photocatalytic degradation performed in acidic conditions removes the thick hydroxylate layer, which causes the attenuation of the photoelectron escaping the Fe_2O_3 particles.

The Fe $2p_{1/2}$ line of the copolymer−Fe_2O_3 sample is very broad and can be deconvoluted into two components with line positions at 710.0 and 711.6 eV. These two components correspond to the Fe^{2+} and Fe^{3+} species,[27] respectively. For the sample after Orange II degradation, the intensity ratio of the Fe^{2+}/Fe^{3+} species was found to be 46:54. Powder Fe_2O_3 used as a reference showed an intensity ratio of 56:44. Hence, the catalyst after Orange II degradation is significantly richer in more positive iron ions than in the reference Fe_2O_3 powder. This observation supports the conclusion that Fe_2O_3 particles participate in oxidation−reduction reactions during Orange II photodegradation.

IR and XPS Characterization of Copolymer−Fe^{3+} before and after Degradation of Orange II. IRATR spectra of copolymer−Fe^{3+} before and after Orange II degradation and the respective band assignments are listed in Table 1. A reflection spectrum of a polymer−Fe^{3+} sample shows the appearance of new bands at 1594, 1560, and 1523 cm^{-1}. These bands are assigned to the asymmetric-stretching vibrations of the carboxylate groups. The new band at 1415 cm^{-1} is due to

TABLE 4: Binding Energy of Fe 2p, O 1s, and C 1s Elements and Atomic Surface Concentration of Detected Elements for Polymer−Fe^{3+} Catalysts

(a) Binding Energy (eV)

sample	Fe 2p	O 1s			C 1s
polymer−Fe^{3+} before use	711.2	532.6	531.3	529.7	284.6
polymer−Fe^{3+} after use in degradation of Orange II	712.0	533.1	531.8	530.2	284.0

(b) Atomic Surface Concentration (%)

		O			
sample	Fe 2p	H_2O_{ads}	OH_{surf}	O_{oxides}	C
polymer−Fe^{3+} before use	4.2	2.9	17.3	4.4	71.4
polymer−Fe^{3+} after use in degradation of Orange II	0.9	4.0	6.3	3.0	86.0

the symmetric-stretching vibrations of the carboxylate groups. Concomitantly, the band at 1793 cm^{-1} assigned to carboxyl anhydride almost disappears. These observations indicate that an iron−carboxylate surface complex is formed. The bands at 1560 and 1523 cm^{-1} have positions similar to those observed in the copolymer−Fe_2O_3 samples, and the peak assignment follows what has been reported in the previous section. The additional band at 1594 cm^{-1} is due to the formation of a carboxylate complex with iron bonded to the OH group. The higher position of asymmetric vibration indicates that a more covalent bonding is taking place. The formation of mixed-valence $Fe^{2+}-Fe^{3+}$ complexes could also be considered. The strongest bands due to the asymmetric and symmetric stretching of carboxylate groups are observed at 1594 and 1415 cm^{-1}, respectively. The calculated $\Delta\nu$ parameter is 179 cm^{-1} according to the literature and indicates the formation of a surface bridging complex.[25,26] For the lower intensity asymmetric bands at 1560 and 1523 cm^{-1}, the calculated $\Delta\nu$ values are 145 and 108 cm^{-1}, indicating chelation or bridging. It should be noted that only one band of the symmetric-stretching vibration bands of the $-COO^-$ groups is observed in the reflection spectrum. Other symmetric-vibration bands overlap with the strong CH_2 deformation bands of the copolymer at 1460 cm^{-1}. This makes the interpretation of the $\Delta\nu$ parameter ambiguous. The band position at about 1460 cm^{-1} is frequently reported as being characteristic of the asymmetric-stretching vibrations of the iron and titanium−carboxylate complexes produced in solution.[25,26] Assuming this possibility, the estimated value of $\Delta\nu$ is 63 cm^{-1}, indicating bridging iron−carboxylate complex formation for the copolymer−Fe^{3+} catalyst. The copolymer−Fe^{3+} samples show a band at 1640 cm^{-1}, indicating a significant water adsorption similar to that of copolymer−Fe_2O_3. Compared to the spectrum of a copolymer−Fe_2O_3 sample, a new broad band at about 829 cm^{-1} and strong bands at ∼3473 and 3363 cm^{-1} are also observed. The latter bands indicate the formation of iron oxide−hydroxide species by the copolymer-loaded sample.[24] The reflection spectrum of copolymer−Fe^{3+} after Orange II degradation shows few differences compared with the spectrum of a freshly prepared sample. A more defined band is found at about 1594 cm^{-1}. This corresponds to a covalent surface carboxylate complex.

The XPS results of copolymer−Fe^{3+} samples before and after Orange II degradation are presented in parts a and b of Table

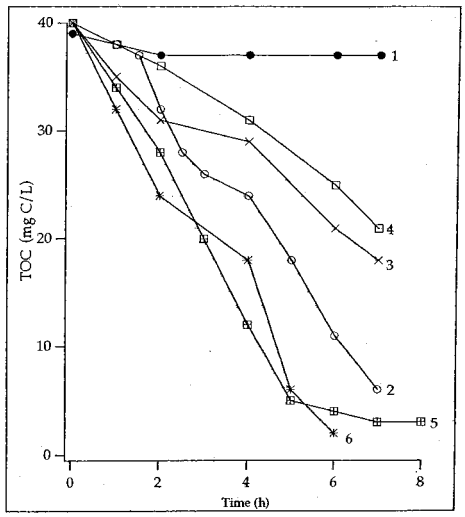

Figure 5. Decrease in TOC of a solution of Orange II (0.2 mM) at a pH of 3 under Suntest irradiation in the presence of H_2O_2. [Traces: (1) copolymer−Fe_2O_3 in the dark and H_2O_2 (10 mM), (2) copolymer−Fe_2O_3 under light and H_2O_2 (10 mM), (3) Fe_2O_3 suspensions of 25 mg/L and H_2O_2 (1 mM), (4) Fe_2O_3 suspensions of 75 mg/L and H_2O_2 (1 mM), (5) Fe_2O_3 suspensions of 25 mg/L and H_2O_2 (10 mM), (6) Fe_2O_3 suspensions of 75 mg/L and H_2O_2 (10 mM).]

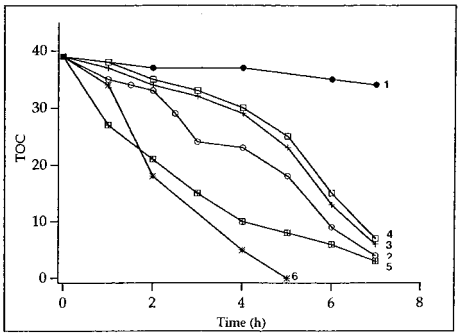

Figure 6. Decrease in TOC for a solution of Orange II (0.2 mM) in the presence of H_2O_2 under Suntest irradiation. [Traces: (1) copolymer−Fe^{3+} and H_2O_2 (10 mM) in the dark, (2) copolymer−Fe^{3+} and H_2O_2 (10 mM) under light, (3) Fe^{3+} (0.2 mM) and H_2O_2 (1 mM) under light, (4) Fe^{3+} (0.5 mM) and H_2O_2 (1 mM) under light, (5) Fe^{3+} (0.2 mM) and H_2O_2 (10 mM) under light, (6) Fe^{3+} (0.5 mM) and H_2O_2 (10 mM) under light.]

4. The most striking difference found is in the intensity of the Fe 2p line observed for copolymer−Fe^{3+} after use. The intensity of the latter band is about 5 times lower compared to the unused copolymer−Fe^{3+}. The low intensity of the Fe 2p line observed in copolymer−Fe^{3+} after Orange II degradation makes it difficult to describe the changes in the Fe oxidation state after use. However, there is a significant difference in the O 1s lines between these two samples. The unused sample shows a much higher surface density of two oxygen components. Particularly, the oxygen-containing peaks related to OH_{surf} (at 533 eV) and to the oxide (at 530 eV) are observed to be weak after Orange II degradation.

Degradation of Orange II on Polymer−Fe_2O_3 and Fe^{3+}−Polymer Films under Suntest Light Irradiation. Figure 5 shows the degradation of Orange II on copolymer−Fe_2O_3 in the dark and under light irradiation. No degradation was observed in the dark, but under light irradiation, ∼90% degradation was completed in ∼7 h. The abatement rate for the copolymer−Fe_2O_3-mediated process was seen to be comparable to a solution containing Fe_2O_3 (75 mg/L) in the presence of H_2O_2 (10 mM). For the other concentrations of hematite with

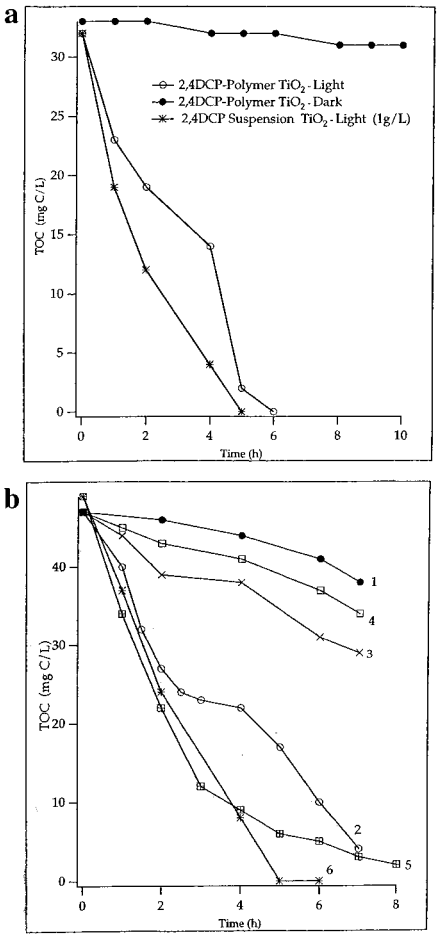

Figure 7. (a) Degradation of 2,4-dichlorophenol (0.5 mM) on copolymer−TiO_2 membranes under medium-pressure mercury-light irradiation at a pH of 6. Solutions were continuously purged with O_2 during irradiation. The TiO_2 content of the suspension was 1 g/L. (b) Decrease in TOC of a solution of 4-chlorophenol (0.65 mM) at a pH of 3 under Suntest light irradiation. [Traces: (1) copolymer−Fe_2O_3 in the dark and H_2O_2 (10 mM), (2) copolymer−Fe_2O_3 under light and H_2O_2 (10 mM), (3) Fe_2O_3 suspensions of 25 mg/L and H_2O_2 (1 mM), (4) Fe_2O_3 suspensions of 75 mg/L and H_2O_2 (1 mM), (5) Fe_2O_3 suspensions of 25 mg/L and H_2O_2 (10 mM), (6) Fe_2O_3 suspensions of 75 mg/L and H_2O_2 (10 mM).]

a 150 m^2/g surface area, the photodegradation results follow what is expected from the concentrations of the catalyst in solution. For the suspensions in Figure 5, the Fe^{3+} to Fe^{2+} redox cycle on copolymer−Fe_2O_3 is suggested as

$$\text{Orange II} + \text{copolymer}-Fe_2O_3 + h\nu \rightarrow [\text{Orange II}^*...Fe_2O_3]\text{copolymer} \rightarrow \text{Orange II}^{\bullet+} + \text{copolymer}-Fe_2O_3 + e^-_{cb} \quad (3)$$

Similar processes for Orange II degradation on Fe_2O_3 powders have been recently reported.[24] No absorption changes were observed on copolymer−Fe_2O_3 after six repetitive degradation cycles. This confirms the stable anchoring between iron oxide and the copolymer film. No Fe^{3+} or Fe^{2+} was detected in solution by thiocyanate or phenanthroline after the runs when using copolymer−Fe_2O_3. The BET surface area of the copolymer−Fe_2O_3-loaded copolymer was 2.77 m^2/g compared to that of the copolymer alone (1.34 m^2/g).

Figure 6 presents the results for copolymer−Fe^{3+}-mediated degradation of Orange II under different experimental conditions. The experimental results follow the trend shown previ-

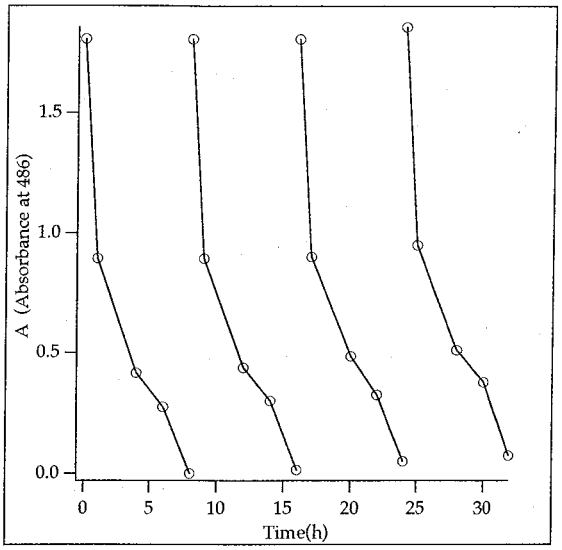

Figure 8. Repetitive mineralization of Orange II (0.1 mM) during the decoloration at a pH of 6 on copolymer−TiO_2 under medium-pressure light irradiation in the presence of H_2O_2 (0.10 mM).

ously in Figure 5 for copolymer−Fe_2O_3 catalysts. The photosensitization of Orange II on copolymer−Fe^{3+} would involve a charge-transfer interaction with the quenching of Orange II

$$\text{Orange II} + \text{Fe}^{3+}\text{−copolymer} + h\nu \rightarrow [\text{Orange II}^{*}...\text{Fe}^{3+}]\text{copolymer} \rightarrow \text{Orange II}^{\bullet+} + \text{Fe}^{2+}\text{−copolymer} \quad (4)$$

The lack of mineralization in the dark compared to light-induced processes in Figure 7bis due to the slow conversion kinetics of Fe^{3+} to Fe^{2+}.[2,14]

Degradation of Chlorophenols by Copolymer−TiO_2 and Copolymer−Fe_2O_3. Figure 7a presents the mineralization of 2,4-DCP under mercury-light irradiation at an initial pH of 6. Under light irradiation, the mineralizations in the titania suspensions and the copolymer−TiO_2 films are seen to proceed at comparable rates. This shows the advantage of using copolymer−TiO_2 instead of TiO_2 suspensions because the fixed titania avoids the separation of the catalyst in suspension at the end of the treatment. In the dark, no mineralization was observed, as indicated by the upper traces of Figure 7a. No H_2O_2 was used as an electron acceptor because the continuous purging with O_2 was sufficient to enhance the charge separation at the TiO_2 surface

$$(O_2)_{ads} + e^-_{cb} \rightarrow (O_2^{\bullet-})_{ads} \quad (5)$$

The pH during 2-chlorophenol mineralization decreased from 6.0 to 4.0 resulting from the production of HCl as shown below

$$\text{HO−}C_6H_3\text{−}Cl_2 + 6O_2 \rightarrow 6CO_2 + H_2O + 2HCl \quad (6)$$

H_2O_2 generated in the solution was observed to remain at a level of ∼0.5 mg/L. The formation of peroxide in TiO_2 suspensions under light has been widely reported in the literature.[7] Figure 7a shows that the mineralization kinetics of 2,4-DCP on titania suspensions or with copolymer−TiO_2 are about the same. The copolymer had a loading of 1.5 mg of TiO_2 on a polymer surface area of 48 cm^2. The amount of titania in the suspension was 40 mg/40 mL, which makes it ∼27 higher than the titania bound on the copolymer surface. The poor performance observed in suspensions could be ascribed to the screening effect of the incoming light by the titania suspension. This is not the case for the transparent copolymer−TiO_2. The photo-oxidation of halocarbons and other organic pollutants on TiO_2 thin films supported on glass or silica paper has been recently reported and is an area of current interest. Recent work by Heller and Brock,[30] Fujishima et al.,[31] Pichat and Ceulemans,[32] and Zahraa et al.[33] have addressed the problem of the deposition of TiO_2 on suitable inorganic supports.

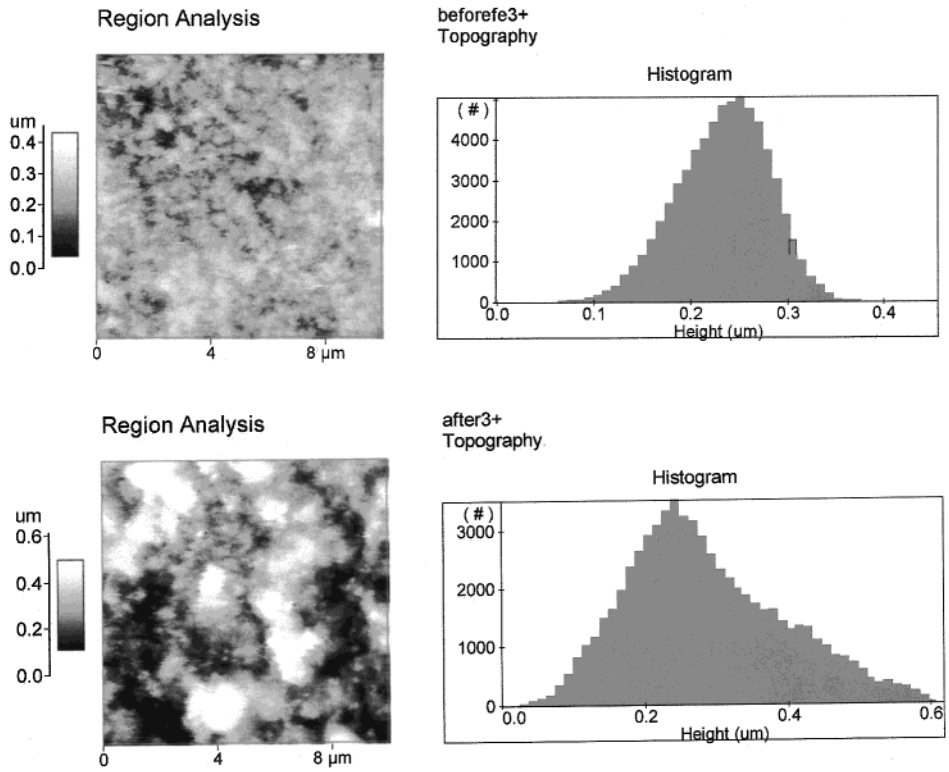

Figure 9. Atomic force microscopy showing the copolymer−Fe^{3+} sample before and after catalyzing the degradation of Orange II.

To check the stability of copolymer−TiO_2 during the reaction, ICPS was carried out to determine the amount of TiO_2 released as a fine particulate into the solution (which is equivalent to the amount of Ti^{4+} ions). The concentration of Ti^{4+} ions in solution after eight recyclings of the copolymer−TiO_2 catalyst varied between 0.14 and 0.50 ppm of Ti^{4+} ion. This is far below the upper limit set by the European Directive (for details see ref 34) allowing up to 5 ppm of Ti^{4+} in aqueous solutions. Furthermore, Ti^{4+} has been reported to be nontoxic up to very high levels.[1,3,5] The fact that we have practically not found any titania in solution after the catalytic run confirms that, for copolymer−TiO_2, TiO_2 is chemically bonded to the surface of the polymer via carboxylic groups. IR data provided evidence that the conjugated carboxylic groups of the maleic anhydride strongly interact with Ti^{4+}. The structure of this bonding would involve two Ti^{4+} ions binding to one carboxylic group. Such a structure has been worked out for 2,2′-bipyridylruthenium(II) complexes chelating the TiO_2 surface.[29] Copolymer−TiO_2 was observed to be stable in acidic as well as basic media up to a pH of 9.

Figure 7b shows the photodegradation of 4-chlorophenol on copolymer−Fe_2O_3. Experiments with copolymer−Fe_2O_3 films in the dark show a reduction in TOC of ∼10%. However, under light irradiation, degradation of 4-chlorophenol reached ∼90% within 7 h. Experiments varying the amount of Fe_2O_3 in the suspensions and the concentration of H_2O_2 in solution are shown in traces 3−6. The trend in Figure 7b followed the results in Figure 7a. Very few studies are available on the iron oxide-mediated degradation of halocarbons.[1,2,7,14,18,35] Cunningham and Sedlak[36] have investigated the degradation of oxalic acid on hematite and found that the process was rather inefficient.

Catalytic Nature of the Photodegradation of Orange II on Copolymer−TiO_2. Figure 8 presents the cyclic repetitive decoloration of Orange II on copolymer−TiO_2. At the end of each cycle, the polymer was washed and Orange II (0.2 mM) and H_2O_2 were added into the solution. The results in Figure 8 confirm the photocatalytic nature of Orange II degradation on supported catalyst. No measurable amounts of Ti^{4+} were found after each cycle in the solution.

TEM and BET Areas. Electron microscopy of copolymer−TiO_2 revealed that the TiO_2 particle size more frequently observed was in the range of 20−30 nm. The diffraction pattern of TiO_2 showed anatase as the main phase and rutile as the secondary phase. The ratio between the two phases corresponds to the known ratio in Degussa P-25 of 80:20. The electron diffraction was carried out to confirm the Degussa P-25 crystallographic structure of the titania bound on the copolymer. The particles of TiO_2 on the copolymer were seen to form a protecting compact layer. No significant change in the BET surface area of the loaded (1.45 m^2/g) compared to the unloaded (1.34 m^2/g) copolymer film was observed.

Atomic Force Microscopy of Copolymer Samples. The histograms of fresh copolymer−Fe^{3+} samples are shown in the upper part of Figure 9, and the samples after mediating the photodegradation of Orange II are in the lower part of this figure. These histograms refer to the selected areas shown to the left in Figure 9. The average roughness for the unused sample was 385 Å, and for the sample after use, the value found was 881 Å. The increase in roughness (root-mean-square value) of the used samples indicates that the catalyst has become more porous. For the copolymer−Fe_2O_3 catalyst, no meaningful difference was found for the roughness because a value of 551 Å after photodegradation was observed versus a roughness factor of 507 Å for samples before use. The change in the roughness for the copolymer−TiO_2 samples was observed to be considerable: 658 Å after use and 568 Å before use. This was the only change observed in the catalysts after repetitive recycling.

Conclusions

This study indicates that the azo-dye Orange II and chlorocarbons can be decolored and degraded via photocatalysis on TiO_2 and Fe_2O_3 immobilized on modified copolymer films. The degradation of Orange II is shown to depend on the type of the model organic compound used, the physical characteristics of the bound semiconductor, the type of scavenger chosen for the separation of the charges on the semiconductor surface, and the irradiation source. No catalyst deposited on the polymer surface leaches out during degradation. IR spectroscopy data also provides evidence that the conjugated carboxylic groups of the maleic anhydride strongly interact with Ti^{4+}. The bands observed by IR also show the high stability of the polymer surface. XPS analysis confirms the intervention of supported Fe_2O_3 during redox processes on the copolymer surface during Orange II photodegradation. By XPS, it was not possible to detect the absorption of intermediates on the catalyst surface after photocatalysis, indicating an adequate catalytic activity of the new materials. The performance of the immobilized photocatalysts was shown to be comparable to semiconductor suspensions with a higher semiconductor loading per unit volume of solution. This effect is due to the absence of the screening effect between the catalyst particles when they are dispersed on thin films.

Acknowledgment. We thank KTI/CTI TOP NANO 21 for financial support under Grant No. 4823. The authors also thank J. Lambert for his technical assistance with the XPS part of this study.

References and Notes

(1) Halmann, M. *Photodegradation of Water Pollutants*; CRC Press: Boca Raton, FL, 1996.
(2) Bauer, R.; Waldner, G.; Fallmann, H.; Hager, S.; Klare, M.; Malato, S.; Maletzky, P. *Catal. Today* **1999**, *53*, 131.
(3) Pitter, P.; Chudoba, J. *Biodegradability of Organic Substances in the Aquatic Environment*; CRC Press: Boca Raton, FL, 1990.
(4) Lucarelli, L.; Nadtochenko, V.; Kiwi, J. *Langmuir* **1999**, *16*, 1102.
(5) Acher, J.; Rosenthal, I. *Water Res.* **1997**, *1111*, 557.
(6) Zhang, F.; Zhao, J.; Hidaka, H.; Pelizzetti, E.; Serpone, N. *Appl. Catal., B* **1998**, *15*, 147.
(7) Ollis, F. D.; Al-Ekabi, H. *Photocatalytic Purification of Water and Air*; Elsevier: Amsterdam, The Netherlands, 1993.
(8) Mills, A.; Morris, S. *J. Photochem. Photobiol., A* **1993**, *71*, 285.
(9) Hofstadler, K.; Bauer, R.; Novalic, S.; Heisler, G. *Environ. Sci. Technol.* **1994**, *28*, 670.
(10) Minero, C.; Pelizzetti, E.; Sega, M.; Vincenti, M. *Environ. Sci. Technol.* **1996**, *29*, 2226.
(11) Korman, C.; Bahneman, D.; Hoffmann, M. *J. Photochem. Photobiol., A* **1989**, *48*, 161.
(12) Stafford, U.; Gray, K. A.; Kamat, P. V. *J. Phys. Chem.* **1994**, *98*, 6343.
(13) Al-Ekabi, H.; Serpone, N. *J. Phys. Chem.* **1988**, *92*, 5276.
(14) Fernandez, J.; Bandara, J.; Lopez, A.; Buffat, Ph.; Kiwi, J. *Langmuir* **1999**, *15*, 185.
(15) Thampi, K. R. EPFL Patent Application, 2000.
(16) Dhananjeyan, M. R.; Kiwi, J.; Thampi, K. R. *Chem. Commun.* **2000**, 1443.
(17) Shirley, A. *Phys. Rev.* **1979**, *B5*, 4709.
(18) Harrick, N. J. *Internal Reflection Spectroscopy*; Interscience Publishers: New York, 1987.
(19) Vinogpodal, K.; Kamat, P. *J. Photochem. Photobiol., A* **1994**, *10*, 1767.
(20) Bandara, J.; Kiwi, J. *New J. Chem.* **1999**, *23*, 717.
(21) Turro, N. J. *Modern Molecular Photochemistry*; University Science Books: Sausalito, CA, 1991.

(22) Bellamy, L. J. *Infrared Spectra of Complex Molecules*; Chapman & Hall: New York, 1975.
(23) Colthup, J. *J. Opt. Soc. Am.* **1950**, *40*, 397.
(24) Bandara, J.; Mielzcarski, J.; Kiwi, J. *Langmuir* **1999**, *15*, 7680.
(25) Deacon, G. B.; Philips, R. J. *Coord. Chem. Rev.* **1980**, *33*, 227.
(26) Mehrotra, R. C.; Bohra, R. *Metal Carboxylates*; Academic Press: New York, 1983.
(27) *Handbook of X-ray Photoelectron Spectroscopy*; Mullenberg, G. E., Ed.; Perkin-Elmer Corp.: Eden Prairie, MN, 1985.
(28) Mielczarski, J. A.; Mielczarski, E. *J. Phys. Chem.* **1995**, *99*, 3206.
(29) Nazeeruddin, Md. K.; Zakeeruddin, S. M.; Humphry-Baker, R.; Shklover, V.; Fisher, C.-H.; Grätzel, M. *Inorg. Chem.* **1999**, *38*, 6298.
(30) Heller, A.; Brock, J. U.S. Patent 4,997,576, March 5, 1991.
(31) Kikuchi, Y.; Sunada, K.; Hashimoto, K.; Fujishima, A. *J. Photochem. Photobiol., A* **1997**, *106*, 51 and references therein.
(32) Ceulemans, E.; Pichat, P. *Abstract*, Chimie, Soleil, Energie, et Environnement, Saint-Avold, France, Feb 2000; p 22.
(33) Zahraa, O.; Chen, H.; Dorion, C.; Bouchy, M. *Abstract*, Chimie, Soleil, Energie, et Environnement, Saint-Avold, France, Feb 2000; p 42.
(34) Valandro, V.; Betti, R. *J. Environ. Pathol. Toxicol. Oncol.* **1997**, *16*, 163.
(35) Lausanne Workshop on Advanced Oxidation Technologies, Lausanne, Switzerland, Oct 1998.
(36) Cunningham, J.; Sedlak, P. *J. Photochem. Photobiol., A* **1994**, *77*, 255.